

1-1-2026

Influence of Solvent Type on the Morphology and Mechanical Properties of Electrospun PMMA Nanofibers

Mohd Khairulniza Mansor

*Faculty of Applied Sciences, Universiti Teknologi MARA, 40450 Shah Alam, Selangor Malaysia AND
Technology & Engineering Division, Malaysian Rubber Board, 47000 Sungai Buloh, Selangor, Malaysia,
mkhairulniza@gmail.com*

Ahmad Faiza Mohd

*Faculty of Applied Sciences, Universiti Teknologi MARA, 40450 Shah Alam, Selangor Malaysia AND
Institute of Science, Universiti Teknologi MARA, 40450 Shah Alam, Selangor Malaysia,
ahmadfaiza@uitm.edu.my*

Khairunnadim Ahmad Sekak

*Faculty of Applied Sciences, Universiti Teknologi MARA, 40450 Shah Alam, Selangor Malaysia,
nadim821@uitm.edu.my*

Norhanifah Mohd Yazid

*Technology & Engineering Division, Malaysian Rubber Board, 47000 Sungai Buloh, Selangor, Malaysia,
norhanifah@lgm.gov.my*

Nurul Fatahah Asyqin Zainal

*Centre of Foundation Studies, Universiti Teknologi MARA, Cawangan Selangor, Kampus Dengkil, 43800
Dengkil, Malaysia, nurulfa2916@uitm.edu.my*

Follow this and additional works at: <https://bsj.uobaghdad.edu.iq/home>

See next page for additional authors

How to Cite this Article

Mansor, Mohd Khairulniza; Mohd, Ahmad Faiza; Ahmad Sekak, Khairunnadim; Mohd Yazid, Norhanifah; Zainal, Nurul Fatahah Asyqin; and Chong, Yong Kok (2026) "Influence of Solvent Type on the Morphology and Mechanical Properties of Electrospun PMMA Nanofibers," *Baghdad Science Journal*: Vol. 23: Iss. 1, Article 4.

DOI: <https://doi.org/10.21123/2411-7986.5150>

This Special Issue Article is brought to you for free and open access by Baghdad Science Journal. It has been accepted for inclusion in Baghdad Science Journal by an authorized editor of Baghdad Science Journal.

Influence of Solvent Type on the Morphology and Mechanical Properties of Electrospun PMMA Nanofibers

Authors

Mohd Khairulniza Mansor, Ahmad Faiza Mohd, Khairunnadim Ahmad Sekak, Norhanifah Mohd Yazid, Nurul Fatahah Asyqin Zainal, and Yong Kok Chong



SPECIAL ISSUE ARTICLE

Influence of Solvent Type on the Morphology and Mechanical Properties of Electrospun PMMA Nanofibers

Mohd Khairulniza Mansor^{1,3}, Ahmad Faiza Mohd^{1,2,*},
Khairunnadim Ahmad Sekak¹, Norhanifah Mohd Yazid³,
Nurul Fatahah Asyqin Zainal⁴, Yong Kok Chong³

¹ Faculty of Applied Sciences, Universiti Teknologi MARA, 40450 Shah Alam, Selangor Malaysia

² Institute of Science, Universiti Teknologi MARA, 40450 Shah Alam, Selangor Malaysia

³ Technology & Engineering Division, Malaysian Rubber Board, 47000 Sungai Buloh, Selangor, Malaysia

⁴ Centre of Foundation Studies, Universiti Teknologi MARA, Cawangan Selangor, Kampus Dengkil, 43800 Dengkil, Malaysia

ABSTRACT

Electrospinning is a versatile and widely used technique for producing nanofibers with controlled morphology and high surface area, essential for applications in filtration, biomedical engineering, and sensors. The choice of solvent plays a crucial role in determining the efficiency of the electrospinning process and the properties of the resulting fibers. In this study, poly(methyl methacrylate) (PMMA) nanofibers were fabricated *via* electrospinning using four different solvents: tetrahydrofuran (THF), dimethylformamide (DMF), chloroform (CHCl₃), and acetone at a 20% (w/w) polymer concentration. Surface tension tests revealed that DMF exhibited the highest surface tension, at 40.11 mN/m, which influenced fiber formation. Electrospinning parameters were optimized, and the nanofibers were characterized using Field Emission Scanning Electron Microscopy (FESEM) and Atomic Force Microscopy (AFM). FESEM confirmed nanofiber diameters ranging from 100 nm to 700 nm, with DMF-based fibers showing the smallest average diameter (~150 nm). AFM analysis revealed that DMF-PMMA nanofibers exhibited the highest surface roughness, which can be attributed to the solvent properties. These results demonstrate that DMF is the most effective solvent among those tested for producing fine PMMA nanofibers with superior morphology and enhanced surface characteristics, underscoring the critical impact of solvent selection in electrospinning nanofiber fabrication.

Keywords: Electrospinning, Nanofiber, Poly(methyl methacrylate), Solvents, Surface tension

Introduction

Nanotechnology is an emerging field and is recognized as a crucial scientific and commercial enterprise with significant worldwide economic advantages. Due to the growing understanding of nanomaterial fabrication techniques, research organizations worldwide increasingly prioritise developing nanomaterials for diverse applications. The methods include drawing-processing, template-assisted synthesis, self-

assembly, solvent casting, phase separation, and electrospinning.^{1–4} The method of electrospinning enables the production of polymeric and inorganic fibres of sizes ranging from micrometers to nanometers.

The electrospinning process begins with the electrification of the droplet, which is extruded from the syringe needle.^{5,6} The droplet is expected to undergo deformation, resulting in a conical shape known as a Taylor cone. When the electrostatic forces exceed

Received 26 February 2025; revised 25 May 2025; accepted 16 June 2025.
Available online 1 January 2026

* Corresponding author.

E-mail addresses: mkhairulniza@gmail.com (M. K. Mansor), ahmadfaiza@uitm.edu.my (A. F. Mohd), nadim821@uitm.edu.my (K. A. Sekak), norhanifah@lgm.gov.my (N. M. Yazid), nurulfa2916@uitm.edu.my (N. F. A. Zainal), kcyong@lgm.gov.my (Y. K. Chong).

International Conference on Discoveries in Applied Sciences and Applied Technology (DASAT2025)

<https://doi.org/10.21123/2411-7986.5150>

2411-7986/© 2026 The Author(s). Published by College of Science for Women, University of Baghdad. This is an open-access article distributed under the terms of the Creative Commons Attribution 4.0 International License, which permits unrestricted use, distribution, and reproduction in any medium, provided the original work is properly cited.

the surface tension of the droplet, a liquid jet is ejected and extends in a linear fashion, resulting in the formation of a droplet at the needle. A static Direct Current (DC) high voltage is typically applied between the needle (syringe) and the conductive collector to create the electric field.⁷ The solvent facilitates the evaporation of the polymeric solution, resulting in the stretching of the jet into finer diameters. This process leads to rapid solidification, culminating in the deposition of long, thin threads onto the grounded collector.^{8,9} The solvent in the polymer solution evaporates during the jet's travel, resulting in the formation of long, thin nanofibers that are collected on a grounded collector. The properties of the solvent, such as surface tension, viscosity, and evaporation rate, play a pivotal role in determining the success of the electrospinning process.¹⁰ For instance, solvents with high surface tension may inhibit the formation of a stable Taylor cone, leading to unstable fiber formation. On the other hand, solvents with low viscosity can result in fibers that are too thin, potentially leading to fiber breakage.^{2,11–13} Additionally, the evaporation rate of the solvent affects the rate of solidification of the fibers, which in turn influences their morphology. Thus, careful selection of the solvent is critical for achieving uniform and high-quality electrospun fibers.

Polymethyl methacrylate (PMMA) has been widely used in electrospinning due to its desirable properties such as optical transparency, mechanical strength, and biocompatibility.^{14,15} PMMA is particularly valued in applications where optical clarity and strength are crucial, such as in tissue scaffolding and drug delivery systems.^{16,17} Despite its widespread use, the electrospinning of PMMA presents challenges in achieving uniform fiber morphology and desirable mechanical properties, making the choice of solvent an important factor in optimizing the electrospinning process. Research has shown that the solvent used during electrospinning can significantly influence the diameter, alignment, and porosity of PMMA nanofibers, directly affecting their performance in specific applications.^{9,16,18}

A number of studies have explored the impact of different solvents on the electrospinning of PMMA. For example, Li et al. (2014)¹⁹ investigated the use of solvents such as dichloromethane (DCM), acetone, chloroform, and tetrahydrofuran (THF) in electrospinning PMMA and demonstrated that solvent properties such as volatility and viscosity influenced the formation of uniform fibers with different cross-sectional shapes. However, despite the extensive body of research, a gap remains in understanding how specific solvent properties (e.g., surface tension, viscosity, evaporation rate) influence the electro-

spinning of PMMA nanofibers in a comprehensive manner. Moreover, while previous studies have explored a variety of solvents, there has been limited focus on optimizing solvent selection to achieve the smallest possible fiber diameter and best mechanical properties.

The aim of this study is to investigate the influence of various solvents, namely THF, dimethylformamide, chloroform, and acetone, on the electrospinning of PMMA nanofibers. This study aims to fill the gap in the existing literature by providing a detailed analysis of how these solvent properties specifically impact the electrospinning process, the resulting fiber morphology, and their potential applications. Furthermore, this research will critically assess the importance of selecting the most effective solvent to produce uniform, high-quality PMMA nanofibers for advanced applications, such as in filtration, tissue engineering, and drug delivery systems.

Materials and methodology

PMMA with distinct molecular weights, $M_w = 120,000 \text{ g}\cdot\text{mol}^{-1}$, and several solvents—Acetone (Ac) $\text{C}_3\text{H}_6\text{O}$, Chloroform (CHCl_3), N, N-dimethylformamide (DMF), and tetrahydrofuran (THF)—were acquired from Sigma Aldrich, Dorsen, UK. The polymer concentration of PMMA utilised throughout this study was 20 wt% relative to the solvents. The polymer solutions were stirred for 4 hours at 60°C , utilising a heating plate (IKA RCT basic, Staufen, Germany), to obtain a transparent solution that demonstrated the complete dissolution of the polymer powder.

Electrospinning setup (ES)

A typical electrospinning system, as shown in Fig. 1, consists of three fundamental components: a high voltage power supply, a capillary tube with a needle,

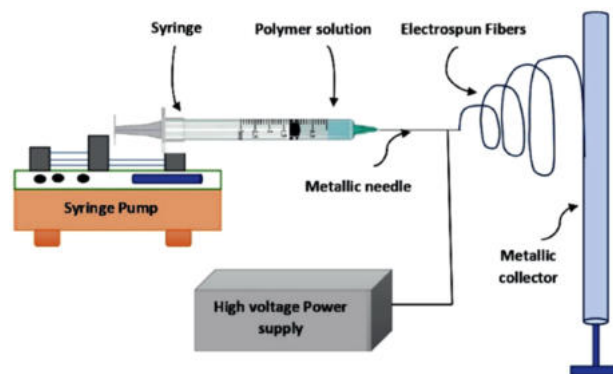


Fig. 1. Electrospinning diagram.⁴

and a collecting screen.¹⁹ In this study, the parameter was meticulously defined as follows: the voltage supply is maintained at a constant value of 15 kilovolts, and the flow rate is determined at 0.5 ml/hr. The syringe had a volume of 3 cc with an 18G needle diameter. The tip-to-collector distance was fixed at 10 cm. All experiments were performed at a controlled room temperature of $25 \pm 2^\circ\text{C}$ and relative humidity of $45 \pm 5\%$, as these conditions influence fiber morphology. The PMMA concentration was constant at 20% w/w.

Surface tension

The KRUSS DSA100HP optical measurement system includes the KRUSS DSA100 Droplet Shape Analyser and the EuroTechnica PD-E1700 high-temperature high-pressure (HTHP) gas/liquid supply device. This system is utilised for MMP measurements of the CO_2/oil system and the $\text{CO}_2/\text{oil}/\text{water}$ system.² The chamber temperature is monitored using a thermocouple (Thermoexpert), which has an uncertainty of 0.2°C at an ambient temperature of 80°C . The system pressure is assessed with a built-in pressure gauge (Armaturenbaubau GmbH), calibrated to an accuracy of 0.1% within the range of 0–100 MPa.

Apparent viscosity

The measurements for all the solvents were conducted utilising a Brookfield rotational viscometer model DV-1, which is presently produced by AMTEK. The device achieves measurements with a precision of $\pm 1\%$ of the range by utilising a spindle of type 2 and measuring speeds of 30 rpm and 60 rpm. The Brookfield DV-1 viscometer provides viscosity measurements in centipoise or millipascal-seconds (mPa·s). All viscosity tests were performed at room temperature (approximately 25°C) to ensure consistent and comparable results.

Gel permeation chromatography (GPC)

A polymer electrospun fibre solution was created by dissolving it in THF and then passing it through a $0.45 \mu\text{m}$ PTFE membrane filter. The rubber's number average molecular weight (M_n), weight average molecular weight (M_w), and polydispersity (M_w/M_n) were determined using GPC (TOSOH HLC-8320GPC) equipped with two TSKgel SuperMultipore HZ-M columns, a RI detector, and a UV detector (UV-8320). The experiment was conducted at a temperature of 30 degrees Celsius, using a flow rate of 0.5 millilitres per minute

for THF. The molecular weight was determined by comparing it to the polystyrene calibration curve.

Field emission scanning electron microscopy (FESEM)

The test portion of the electrospun fibre samples was sectioned and affixed onto the specimen stub using carbon double-sided tape. The specimen was subsequently prepared for inspection. Through the process of evaporative coating, a remarkably thin layer of platinum is applied under conditions of high vacuum. This layer allows for SEM studies by providing conductivity. The specimen underwent analysis with the JEOL JSM-7601F Plus, a field emission scanning electron microscope (FESEM). The FESEM was utilised at an accelerating voltage of 1kV, featuring a working distance of 10 mm and maintaining a tilt angle of 0 degrees. The lower image detector (LEI) was employed for imaging purposes.

Atomic force microscopy (AFM)

The sample obtained from the electrospinning technique was analysed after using the different solvents. The specimen was distributed in isopropyl alcohol (IPA) and thereafter subjected to sonication for approximately 5 minutes. Subsequently, the sample was evenly distributed over the glass slab and allowed to dry at ambient temperature until it reached an adequate state prior to AFM testing. The surface topography of both 2D and 3D was analysed using AFM with a Park System NX-10 (Maxtrom MX-6000EP) instrument. An aluminium-coated cantilever (PPP-NCHR) with a spring constant of 42 N/m was utilised for this purpose. The morphological pictures were obtained using the non-contact mode at a scanning speed of 0.4 Hz over a scan area of $1 \times 1 \mu\text{m}^2$. The average and mean surface roughness (R_a and R_q) were calculated based on three separate regions of interest on the surface of the sample.

Results and discussion

Surface tension

The results of surface tension between solvents are depicted in Figs. 2 and 3. DMF exhibits the highest surface tension among the solvents examined, with a value of 40.11 mN/m. This elevated surface tension promotes the formation of stable polymer jets during electrospinning, leading to the production of well-defined nanofibers with smooth surfaces. Conversely, acetone displays the lowest surface tension at 21.97 mN/m, which may result in the formation of finer

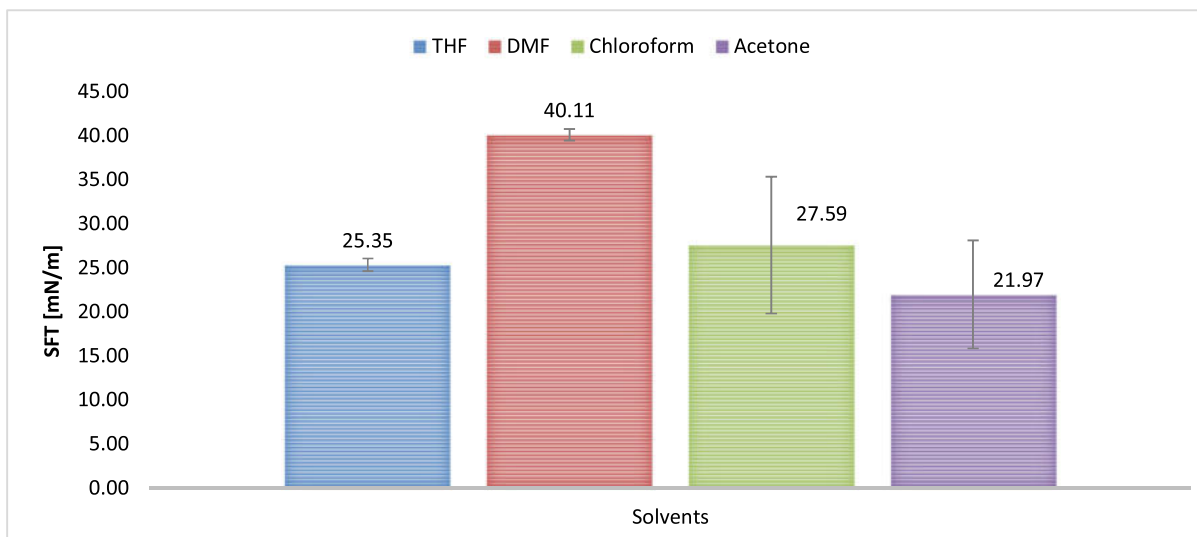


Fig. 2. Surface tension results for analyzed solvents.

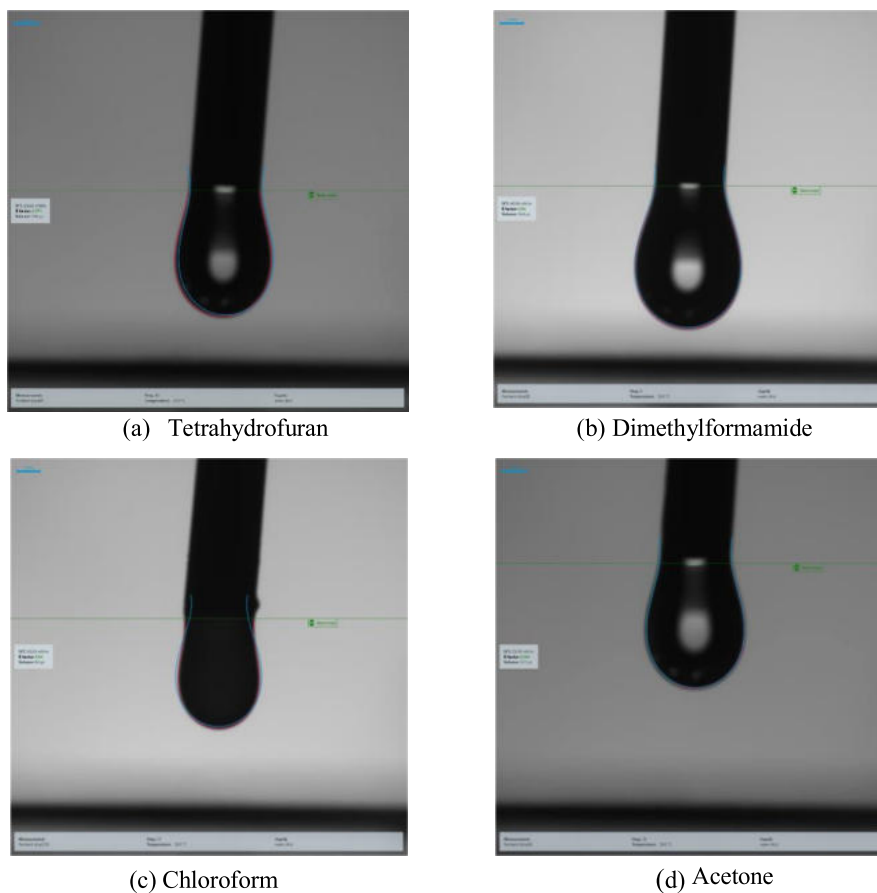


Fig. 3. Surface tension pendant drop images using the Kuss easy drop for various solvents; (a) THF (b) DMF (c) Chloroform and (d) Acetone.

nanofibers due to enhanced stretching and elongation of the polymer solution during electrospinning. THF, with a surface tension of 25.35 mN/m, and chloroform, with a surface tension of 27.59 mN/m, fall within the intermediate range.

A direct correlation is observed between the solvent surface tension and the resulting fiber morphology: higher surface tension solvents tend to produce thicker fibers due to increased cohesive forces that resist jet thinning, whereas lower surface tension

Table 1. Apparent viscosity of polymer solution (20%) using different solvent.

Solvent	Speed (rpm)			Unit
	30	Unit	60	
Tetrahydrofuran-PMMA	17.8 ± 0.4	cP	22.9 ± 0.2	cP
Dimethylformamide-PMMA	56.8 ± 0.4	cP	61.8 ± 0.3	cP
Chloroform-PMMA	19.8 ± 0.4	cP	28.1 ± 0.5	cP
Acetone-PMMA	32.8 ± 1.8	cP	42.6 ± 1.1	cP

solvents facilitate greater jet elongation, resulting in finer fibers.¹¹ However, excessively low surface tension can also destabilize the jet, potentially leading to bead formation or irregular fiber morphology.²⁰ This highlights the importance of selecting solvents with optimal surface tension to achieve a stable jet and uniform fiber formation. Furthermore, the interplay between surface tension and solvent volatility (linked to vapor pressure) critically influences fiber solidification and final morphology solvents with appropriate surface tension and evaporation rates enable controlled fiber formation without defects.^{11,21}

These solvents provide a balance between jet stability and polymer elongation, yielding nanofibers with moderate diameters and structural integrity. Grasping the surface tension characteristics of solvents is crucial for refining electrospinning parameters and managing nanofiber properties for diverse applications, such as tissue engineering, filtration, and drug delivery. The pace at which the solvent evaporates is greatly affected by the vapor pressure of the solvent. The results validate that the physical properties of the polymer are contingent upon the choice of solvent.^{22–24}

Apparent viscosity

Apparent viscosity of 20% PMMA polymer solutions was measured using a Brookfield viscometer, and the results are presented in Table 1, providing insights into their rheological behavior. Among these solvents, DMF-PMMA exhibited the highest viscosity due to strong solvent-polymer interactions that enhance chain entanglement critical for continuous fiber formation. According to entanglement theory, a critical entanglement concentration must be surpassed to form defect-free fibers.²⁵ Chloroform-PMMA follows DMF-PMMA in apparent viscosity due to its lower molecular weight and weaker intermolecular forces. Tetrahydrofuran-PMMA exhibits a moderate apparent viscosity, reflecting its intermediate molecular weight and moderate intermolecular interactions. Lastly, Acetone-PMMA displays the lowest apparent viscosity among the solvents tested, owing to its lower molecular weight and weaker intermolecular forces, resulting in easier flow.

Solutions with viscosity below this threshold (e.g., acetone-PMMA) often yield beaded or non-uniform fibers due to insufficient chain entanglements, while higher viscosity solutions facilitate spindle-like, smooth fibers, as observed with DMF. Increasing polymer solution viscosity promotes alignment and shape transition of electrospun nanofibers from spherical to spindle-like, resulting in smooth fibers with increased diameter. Ultimately, this results in the formation of smooth fibres, although their diameter does increase.^{26–28} Two essential factors involved are the solubility of the polymer in the solvent and the boiling point of the solvent, both of which are vital for ensuring efficient processing. The boiling point is significantly affected by the solvent's volatility.

Other important factors encompass the dipole moment and conductivity of the solvent, which can influence both the electrospinnability of polymer solutions and the morphology of fibres. Jarusuwanapoom et al.²⁹ investigated the impact of 18 solvents on the capacity of polystyrene (PS) solutions to be transformed into fibres. The findings indicated that only five solvents; DMF, THF, ethyl acetate, methyl ethyl ketone, and 1,2-dichloroethane—were suitable for electrospinning. The choice of solvent was determined by the outstanding conductivity and dipole moment of the solvents.^{20,30}

Gel permeation chromatography

Table 2 displays the molecular weight of the fibre produced during the electrospinning process, with variations in solvents and PMMA concentrations at 20% (w/w). The outcome unequivocally demonstrates that the use of DMF as a solvent results in a significantly lower molecular weight of the generated fibre compared to other solvents. This result further corroborated our findings, as the presence of the nanofiber was distinctly observed in the FESEM micrograph. Regarding other solvents, the PMMA 20% solution exhibited a nearly identical average molecular weight distribution. However, it resulted in the production of larger fibre sizes, as observed using FESEM.

Table 2. Molecular weight of electrospun fiber using variation of solvents with 20% PMMA concentration.

Solvent	$M_n \times 10^4$ (g/mol)	$M_w \times 10^4$ (g/mol)	$M_z \times 10^4$ (g/mol)
Tetrahydrofuran	2.77 ± 0.032	6.47 ± 0.031	12.15 ± 0.022
Dimethylformamide	2.38 ± 0.039	5.94 ± 0.083	10.84 ± 0.180
Chloroform	2.73 ± 0.020	6.26 ± 0.042	11.54 ± 0.203
Acetone	2.39 ± 0.045	6.24 ± 0.110	12.29 ± 0.541

In contrast, solvents like Acetone, which showed broader molecular weight distributions, tended to produce nanofibers with larger and more variable diameters. This can be attributed to the presence of higher molecular weight polymer chains within the solution, leading to greater heterogeneity in polymer chain entanglement and solution viscosity. Such variability often results in less uniform fiber formation, as evidenced by the FESEM micrographs.

The relatively narrow and lower molecular weight distribution associated with DMF suggests a more homogeneous polymer chain population, which facilitates consistent chain entanglement during electrospinning.³¹ This promotes the formation of finer and more uniform fibers with controlled diameter and surface properties. Additionally, the low M_z value in DMF solutions indicates fewer large molecular species that can disrupt the jet stability during electrospinning, further contributing to uniform fiber morphology.

Field emission scanning electron microscopy

The scanning electron microscope (SEM) micrograph in Fig. 4 demonstrates the clear morphological and structural features of electrospun nanofibers with a 20% concentration of PMMA, depending on the solvent utilised. When viewed at magnifications between 5,000x and 40,000x, the nanofibers exhibit a uniform and orderly arrangement, forming a dense network on the substrate. In this study, the focus was placed on the comparative morphological analysis of PMMA nanofibers fabricated using different solvents, rather than on quantitative diameter measurement. While quantitative analysis, such as measuring fiber diameters from a large number of samples and generating histograms, can provide detailed statistical insights, the primary objective here was to qualitatively assess the influence of solvent choice on fiber morphology and surface characteristics. Under a magnification of 5000x, the diameters of the fibres in THF, Chloroform, and Acetone vary between approximately $1\mu\text{m}$ and $3\mu\text{m}$. The fibres primarily display an elliptical shape and lack a bead-on-string structure. When DMF is used as a solvent in the process of

electrospinning, the resulting fibre diameters generally range from 200 to 700 nanometers. Future work may include detailed quantitative characterization to complement the present findings.

Occasionally, these fibres may display bead-on-string patterns while maintaining a spherical shape. This implies that DMF demonstrates superior performance compared to other solvents when used under identical electrospinning settings. According to Mo et al.,³² beadlike nanofibres can be produced using electrospinning when the concentration is low. On the other hand, the development of ultrafine nanofibres is more likely to occur at high concentration.³³

These features hold significant implications for applications in tissue engineering and filtration, where precise control over fiber morphology and surface properties plays a crucial role in determining the performance and functionality of the nanofiber-based materials. According to a research report by Jarusuwannapoom et al.,²⁹ the process of spinning polymer in DMF solutions was remarkably effortless, perhaps because of the solvent's relatively high dipole moment and conductivity values. When using a 20% concentration of PMMA, the lowest amount of beaded fibres and the smallest diameter were achieved compared to other solvents. These morphological characteristics have important implications for applications such as tissue engineering and filtration, where fiber uniformity and surface properties critically affect material performance.

Six types of force are to be considered, as explained by Jarusuwannapoom et al.²⁹: (1) gravitational force acting on the body, (2) electrostatic force facilitating the movement of the charged jet from the spinneret to the target, (3) Coulombic force that separates adjacent charged carriers within the jet segment, leading to the stretching of the charged jet during its flight, (4) viscoelastic force that restricts the stretching of the charged jet, (5) surface tension that also counteracts the stretching of the charged jet's surface, and (6) drag force arising from the friction between the charged jet and the surrounding air. Among these forces, only the Coulombic, viscoelastic, and surface tension forces play a role in the formation of beads and the decrease in size of the charged jet as it moves towards the grounded target.

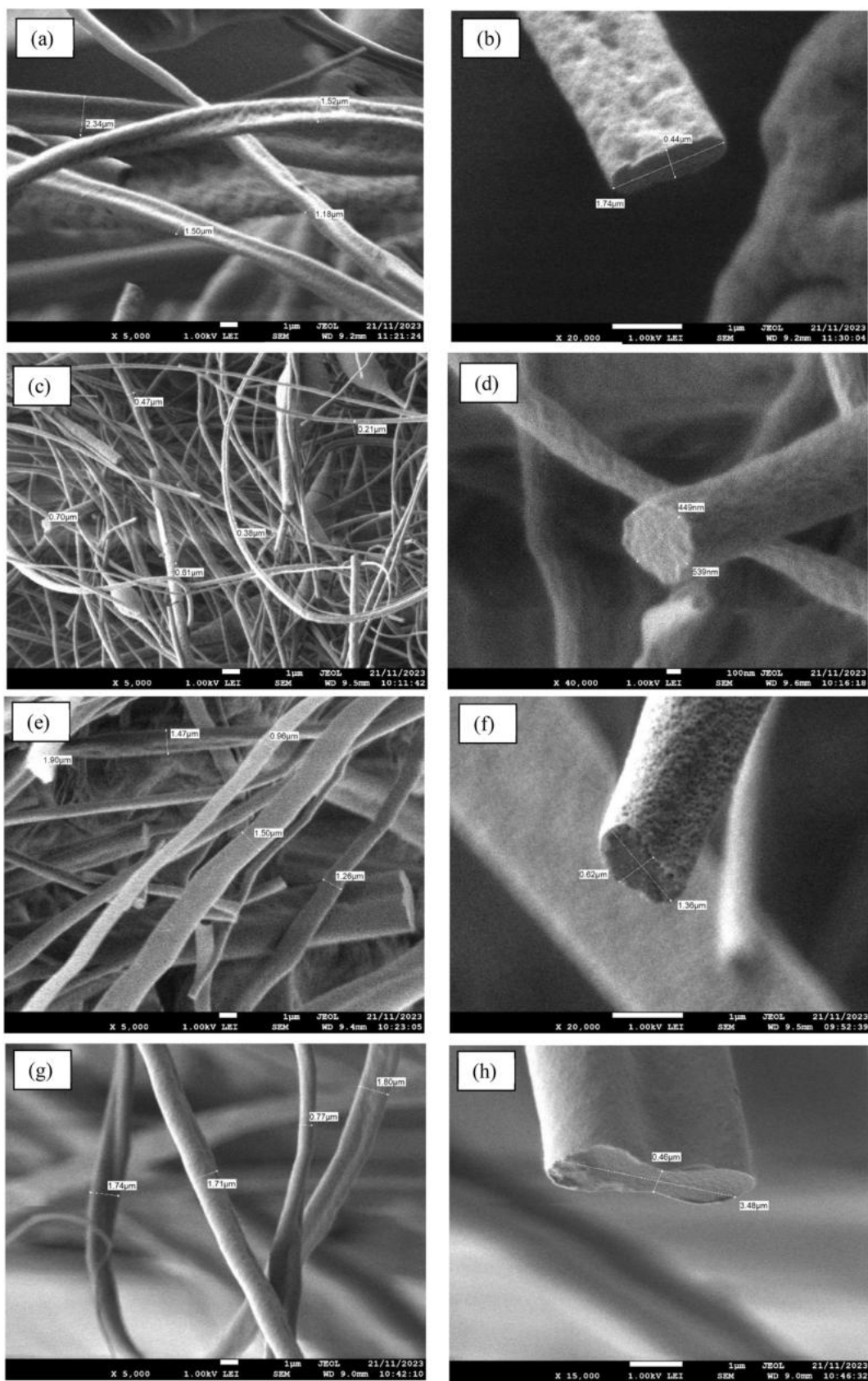


Fig. 4. Micrographs of fibre comparison with difference solvent at low (5000x) and high magnification (15 000- 40 000x). Depict as (a) and (b) Tetrahydrofuran, (c) and (d) Dimethylformamide, (e) and (f) Chloroform, (g) and (h) Acetone.

Atomic force microscopy

A series of PMMA nanofibers in different solvents were produced and characterized regarding their surface roughness and topography. The roughness average (R_a) of the nanofiber surface is tabulated in Table 3. Notably, the R_a of each nanofiber is acknowledged by the solvent used. The surface roughness (R_a) of electrospun PMMA nanofibers is a crucial parameter that influences their performance in various applications. A higher surface roughness generally increases the effective surface area, which can be beneficial for applications such as filtration membranes and sensor interfaces by enhancing interaction sites. Conversely, in biomedical applications like tissue engineering scaffolds, increased roughness often correlates with higher hydrophobicity, potentially reducing cell attachment and proliferation, as supported by previous studies.³⁴ Thus, controlling surface roughness through solvent choice is vital for tailoring nanofiber properties to specific end-uses. It was observed that the DMF-PMMA nanofiber depicted the highest roughness value compared to the other three. Followed by CHCl_3 -PMMA nanofiber. THF-PMMA nanofiber and Ac-PMMA nanofiber are arranged in descending order of roughness average. A rougher surface results in a higher hydrophobicity, which subsequently leads to reduced cell attachment.³⁵

AFM analysis (Table 3) shows that DMF-PMMA nanofibers possess the highest average roughness ($R_a = 6.03 \pm 3.82$ nm), followed by Chloroform ($R_a = 5.19 \pm 0.47$ nm), THF ($R_a = 4.51 \pm 0.32$ nm), and Acetone ($R_a = 3.35 \pm 0.03$ nm). These findings are corroborated by the 3D surface topography images (Fig. 5), where DMF-based fibers reveal a distinct polymer particle arrangement compared to fibers spun from other solvents. The differences in roughness can be attributed to variations in solvent evaporation rates, polymer-solvent interactions, and phase separation dynamics during electrospinning. For instance, slower evaporation of DMF allows more polymer chain mobility, leading to pronounced surface features and roughness.³⁶

The surface topography of all nanofibers is shown in Fig. 5, where (A) 2D- THF-PMMA nanofiber, (B) 2D- DMF-PMMA nanofiber, (C) 2D- CHCl_3 -PMMA nanofiber and (D) 2D-Ac- PMMA nanofiber images following (E) 3D- THF-PMMA nanofiber, (F) 3D-DMF-PMMA nanofiber, (G) 3D- CHCl_3 -PMMA nanofiber (H) 3D-Ac-PMMA nanofiber images at scan area $1 \times 1 \mu\text{m}$. The 2D surface topography illustrates that every solvent used contributes to distinguishing surface topography. The (A) depicted

Table 3. Average roughness of the nanofiber in three different regions.

Sample	THF	DMF	Chloroform	Acetone
R_a (nm)	4.51 ± 0.32	6.03 ± 3.82	5.19 ± 0.47	3.35 ± 0.03
R_q (nm)	5.54 ± 0.49	7.68 ± 4.62	6.58 ± 0.74	4.22 ± 0.11

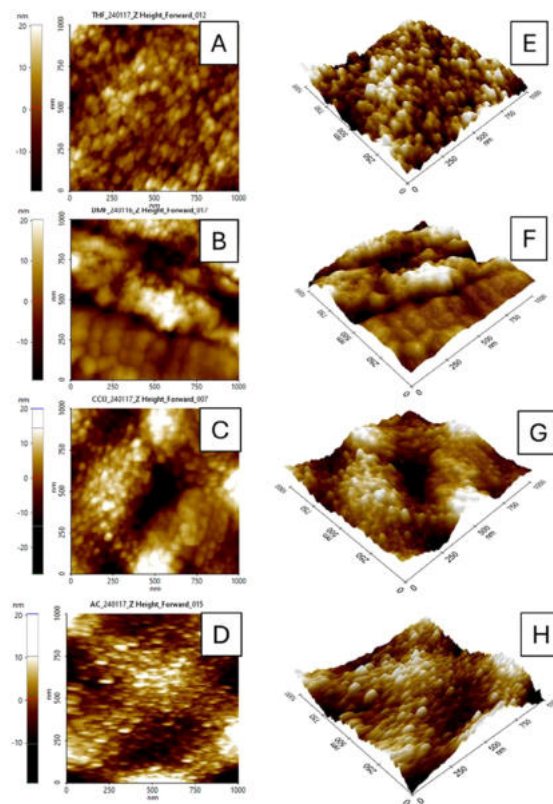


Fig. 5. Atomic force microscopy images of randomly orientated nanofibers with different surface nanoroughness: (A) 2D- THF, (B) 2D-DMF, (C) 2D- CHCl_3 (D) 2D-Acetone images following (E) 3D- THF, (F) 3D-DMF, (G) 3D- CHCl_3 (H) 3D-Acetone images at scan area $1 \times 1 \mu\text{m}$.

the polymer particles in sphere shape in a homogeneous array identical to (C) and (D). Nonetheless, the (B) depicted a different array of polymer particles.

The 3D surface topography confirmed the distinct surface characteristics of each nanofiber. The array of polymer particles influences the R_a value, where the 3D surface topography supports the finding. Furthermore, it is worth mentioning that in Fig. 6, the roughness profile of each nanofiber is clearly distinguishable from the others. Although the array of polymer particles is nearly identical for (A), (C), and (D), the roughness of these nanofibers varies significantly.

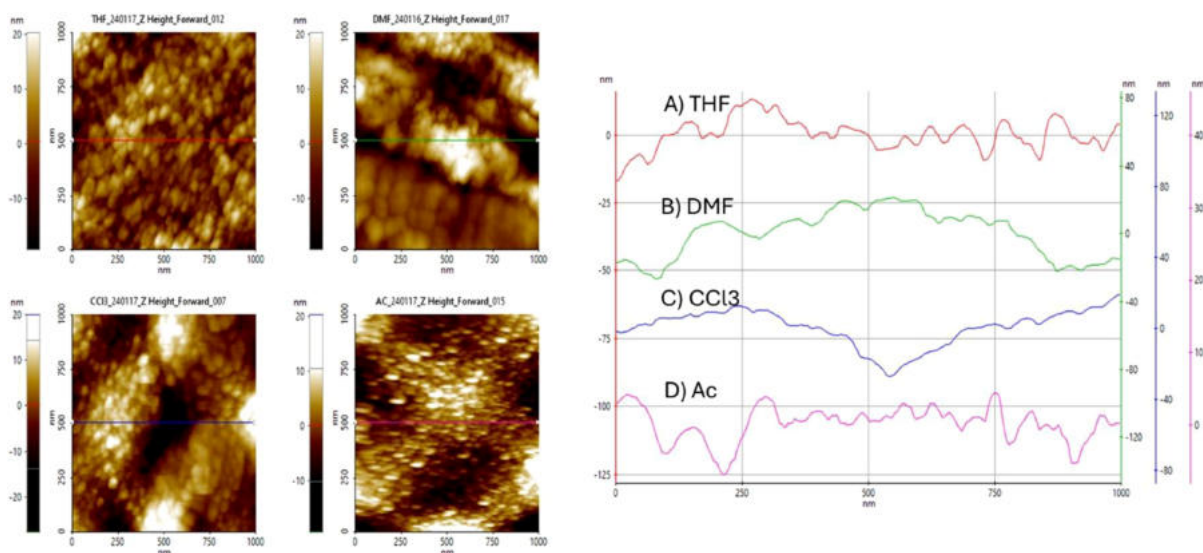


Fig. 6. Roughness profile of A) THF, B) DMF, C) CHCl_3 and D) Acetone.

Conclusion

This study demonstrates that the choice of solvent significantly influences the morphological and surface characteristics of electrospun PMMA nanofibers. Among the solvents tested, DMF produced fibers with the smallest average diameter and highest surface roughness, attributed to its higher viscosity and polymer-solvent interactions. These properties suggest that DMF-PMMA nanofibers could offer enhanced functional performance in applications requiring high surface area and fine fiber networks, such as filtration, sensors, or tissue engineering scaffolds. However, the elevated surface roughness and lower molecular weight average in DMF-based fibers may also impact mechanical strength and cell compatibility, indicating potential limitations that warrant further investigation. Future research should explore optimizing solvent mixtures and electrospinning parameters to balance fiber morphology, mechanical properties, and biocompatibility for targeted applications. Additionally, in-depth studies on the relationship between solvent characteristics, fiber molecular weight distribution, and long-term performance are recommended to advance practical deployment of PMMA nanofibers.

Acknowledgement

The authors express their gratitude to the Faculty of Applied Sciences, MARA University of Technology Malaysia, and the Technology and Engineering Division, Malaysian Rubber Board, for providing the scholarship that supported this research.

Authors' declaration

- Conflicts of Interest: None.
- We hereby confirm that all the Figures and Tables in the manuscript are ours. Furthermore, any Figures and images that are not ours have been included with the necessary permission for republication, which is attached to the manuscript.
- No animal studies are present in the manuscript
- No human studies are present in the manuscript
- Ethical Clearance: The project was approved by the local ethical committee at MARA University of Technology, Shah Alam, Malaysia

Authors' contributions

M.K.M: contributed to data collection, experimental work and setup, methodology, supervision, manuscript drafting and writing, data analysis, and characterization. A.F.M. was responsible for conceptualization, supervision, manuscript drafting, and final editing. K.A.S. did the experimental setup and review of the manuscript. N.M.Y. conducted the experimental setup, material characterization, and review of the manuscript. N.F.A.Z. was responsible for the review of the manuscript. Y.K.C. reviewed the manuscript. All authors have read and approved the final manuscript.

References

1. Smith JA, Mele E. Electrospinning and Additive Manufacturing: Adding Three-Dimensionality to Electrospun Scaffolds for Tissue Engineering. *Front Bioeng Biotechnol.* 2021;9:674738. <https://doi.org/10.3389/fbioe.2021.674738>.

2. Keirouz A, Wang Z, Reddy VS, *et al.* The History of Electrospinning: Past, Present, and Future Developments. *Advanced Materials Technologies*. 2023;8(11):2201723. <https://doi.org/10.1002/admt.202201723>.
3. Shah AA, Yang J, Kumar T, *et al.* Synthesis of transparent electrospun composite nanofiber membranes by asymmetric solvent evaporation process. *Colloids and Surfaces A: Physicochemical and Engineering Aspects*. 2023;666:131264. <https://doi.org/10.1016/j.colsurfa.2023.131264>.
4. Sharma G, James N. Progress in Electrospun Polymer Composite Fibers for Microwave Absorption and Electromagnetic Interference Shielding. *ACS Applied Electronic Materials*. 2021;3 (11), 4657–4680. <https://doi.org/10.1021/acsaelm.1c00827>.
5. Walden R, Aazem I, Hinder S, *et al.* Parametric optimisation of PDMS/PMMA nanofibers prepared using emulsion electrospinning technique. *Results in Materials*. 2024;22:100576. <https://doi.org/10.1016/j.rinma.2024.100576>.
6. Zulfi A, Hartati S, Nur'aini S, *et al.* Electrospun Nanofibers from Waste Polyvinyl Chloride Loaded Silver and Titanium Dioxide for Water Treatment Applications. *ACS Omega*. 2023;8(26):23622-23632. <https://doi.org/10.1021/acsomega.3c01632>.
7. Sivan M, Madheswaran D, Hauzerova S, *et al.* AC electrospinning: impact of high voltage and solvent on the electrospinnability and productivity of polycaprolactone electrospun nanofibrous scaffolds. *Materials Today Chemistry*. 2022;26:101025. <https://doi.org/10.1016/j.mtchem.2022.101025>.
8. Keirouz A, Chung M, Kwon J, *et al.* 2D and 3D electrospinning technologies for the fabrication of nanofibrous scaffolds for skin tissue engineering: A review. *Wiley Interdiscip Rev Nanomed Nanobiotechnol*. 2020;12(4):e1626. <https://doi.org/10.1002/wnan.1626>.
9. Xie Y, Sun X-F, Li W, *et al.* Fabrication of Electrospun Xylan-g-PMMA/TiO₂ Nanofibers and Photocatalytic Degradation of Methylene Blue. *Polymers*. 2022;14(12):2489. <https://doi.org/10.3390/polym14122489>.
10. Al-Okaidy H, Waisi B. The Effect of Electrospinning Parameters on Morphological and Mechanical Properties of PAN-based Nanofibers Membrane. *Baghdad Sci J*. 2023, 20(4): 1433–1441. <https://doi.org/10.21123/bsj.2023.7309>.
11. Ewaldz E, Randrup J, Brettmann B. Solvent Effects on the Elasticity of Electrospinnable Polymer Solutions. *ACS Polymers Au*. 2022;2(2):108–117. <https://doi.org/10.1021/acspolymersau.1c00041>.
12. Shabani A, Al GA, Berri N, *et al.* Electrospinning Technology, Machine Learning, and Control Approaches: A Review. *Advanced Engineering Materials*. 2025;27(7):2401353. <https://doi.org/10.1002/adem.202401353>.
13. Higashi S, Hirai T, Matsubara M, *et al.* Dynamic viscosity recovery of electrospinning solution for stabilizing elongated ultrafine polymer nanofiber by TEMPO-CNF. *Scientific Reports*. 2020;10(1):13427. <https://doi.org/10.1038/s41598-020-69136-2>.
14. Singh AK, Pramod A, J K, *et al.* Electrospun Benzimidazole: Poly(methyl methacrylate) Nanofibers for Optoelectronic Applications. *ACS Applied Optical Materials*. 2024;2(10):2196–2207. <https://doi.org/10.1021/acsaom.4c00346>.
15. Zafar MS. Prosthodontic Applications of Poly-methyl Methacrylate (PMMA): An Update. *Polymers (Basel)*. 2020;12(10):2299. <https://doi.org/10.3390/polym12102299>.
16. Zaszczynska A, Kolbuk D, Gradys A, *et al.* Development of Poly(methyl methacrylate)/nano-hydroxyapatite (PMMA/nHA) Nanofibers for Tissue Engineering Regeneration Using an Electrospinning Technique. *Polymers*. 2024;16(4):531. <https://doi.org/10.3390/polym16040531>.
17. Han X, Lin H, Chen X, *et al.* One-step method for the preparation of poly(methyl methacrylate) modified titanium-bioactive glass three-dimensional scaffolds for bone tissue engineering. *IET Nanobiotechnol*. 2016;10(2):45–53. <https://doi.org/10.1049/iet-nbt.2014.0053>.
18. Xia J, Zheng Z, Guo Y. Mechanically and electrically robust, electro-spun PVDF/PMMA blend films for durable triboelectric nanogenerators. *Composites Part A: Applied Science and Manufacturing*. 2022;157:106914. <https://doi.org/10.1016/j.compositesa.2022.106914>.
19. Li L, Jiang Z, Li M, *et al.* Hierarchically Structured PMMA Fibers Fabricated by Electrospinning. *RSC Adv*. 2014;4(95):52973–52985. <https://doi.org/10.1039/C4RA05385K>.
20. 2Ahmadi Bonakdar M, Rodrigue D. Electrospinning: Processes, Structures, and Materials. *Macromol*. 2024;4(1):58–103. <https://doi.org/10.3390/macromol4010004>.
21. Abdulhussain R, Adebisi A, Conway BR, *et al.* Electrospun nanofibers: Exploring process parameters, polymer selection, and recent applications in pharmaceuticals and drug delivery. *Journal of Drug Delivery Science and Technology*. 2023;90:105156. <https://doi.org/10.1016/j.jddst.2023.105156>.
22. Pashkuleva I, Marques AP, Vaz F, *et al.* Surface modification of starch based biomaterials by oxygen plasma or UV-irradiation. *J Mater Sci Mater Med*. 2010;21(1):21–32. <https://doi.org/10.1007/s10856-009-3831-0>.
23. Cadafalch Gazquez G, Smulders V, Veldhuis SA, *et al.* Influence of Solution Properties and Process Parameters on the Formation and Morphology of YSZ and NiO Ceramic Nanofibers by Electrospinning. *Nanomaterials*. 2017;7(1):16. <https://doi.org/10.3390/nano7010016>.
24. Angel N, Guo L, Yan F, *et al.* Effect of processing parameters on the electrospinning of cellulose acetate studied by response surface methodology. *Journal of Agriculture and Food Research*. 2020;2:100015. <https://doi.org/10.1016/j.jafr.2019.100015>.
25. Bedi JS, Lester DW, Fang YX, *et al.* Electrospinning of poly(methyl methacrylate) nanofibers in a pump-free process. *Journal of Polymer Engineering*. 2013;33(5):453–461. <https://doi.org/10.1515/polyeng-2012-0096>.
26. Huang Z-X, Liu X, Zhang X, *et al.* Electrospun polyvinylidene fluoride containing nanoscale graphite platelets as electret membrane and its application in air filtration under extreme environment. *Polymer*. 2017;131:143–150. <https://doi.org/10.1016/j.polymer.2017.10.033>.
27. Cui J, Li F, Wang Y, *et al.* Electrospun nanofiber membranes for wastewater treatment applications. *Separation and Purification Technology*. 2020;250:117116. <https://doi.org/10.1016/j.seppur.2020.117116>.
28. Doderò A, Brunengo E, Alloisio M, *et al.* Chitosan-based electrospun membranes: Effects of solution viscosity, coagulant and crosslinker. *Carbohydrate Polymers*. 2020;235:115976. <https://doi.org/10.1016/j.carbpol.2020.115976>.
29. Jarusuwannapoom T, Hongrojjanawiwat W, Jitjaicham S, *et al.* Effect of solvents on electro-spinnability of polystyrene solutions and morphological appearance of resulting electrospun polystyrene fibers. *European Polymer Journal*. 2005;41(3):409–421. <https://doi.org/10.1016/j.eurpolymj.2004.10.01030>.
30. Cooper CJ, Mohanty AK, Misra M. Electrospinning Process and Structure Relationship of Biobased Poly(butylene succinate) for Nanoporous Fibers. *ACS Omega*. 2018;3(5):5547–5557. <https://doi.org/10.1021/acsomega.8b00332>.

31. Rajeev M, Helms CC. A Study of the Relationship between Polymer Solution Entanglement and Electrospun PCL Fiber Mechanics. *Polymers (Basel)*. 2023;15(23):4555. <https://doi.org/10.3390/polym15234555>.
32. Mo XM, Xu CY, Kotaki M, *et al*. Electrospun P(LLA-CL) nanofiber: a biomimetic extracellular matrix for smooth muscle cell and endothelial cell proliferation. *Biomaterials*. 2004;25(10):1883–1890. <https://doi.org/10.1016/j.biomaterials.2003.08.042>.
33. Majumder S, Matin MA, Sharif A, *et al*. Electrospinning of antibacterial cellulose acetate/polyethylene glycol fiber with in situ reduced silver particles. *Journal of Polymer Research*. 2020;27(12):381. <https://doi.org/10.1007/s10965-020-02356-2>.
34. Babu A, Aazem I, Walden R, *et al*. Electrospun nanofiber based TENGs for wearable electronics and self-powered sensing. *Chemical Engineering Journal*. 2023;452:139060. <https://doi.org/10.1016/j.cej.2022.139060>.
35. Can-Herrera LA, Oliva AI, Dzul-Cervantes MAA, *et al*. Morphological and Mechanical Properties of Electrospun Polycaprolactone Scaffolds: Effect of Applied Voltage. *Polymers*. 2021;13(4):662. <https://doi.org/10.3390/polym13040662>.
36. Diwan T, Abudi ZN, Al-Furaiji MH, *et al*. A Competitive Study Using Electrospinning and Phase Inversion to Prepare Polymeric Membranes for Oil Removal. *Membranes*. 2023;13(5):474. <https://doi.org/10.3390/membranes13050474>.

تأثير نوع المذيب على الشكل المورفولوجي والخصائص الميكانيكية للألياف النانوية المصنوعة بتقنية الغزل الكهربائي من بولي ميثيل ميثاكريلات (PMMA)

محمد خير النزا منصور¹، أحمد فايزة محمد¹،²، خير النديم أحمد سكاك¹، نور حنيفة محمد يازيد⁴، نور الفتاحه أشقين زينال³،
يونغ كوك تشونغ⁴

¹كلية العلوم التطبيقية، جامعة مارا للتكنولوجيا (UiTM) ، 40450 شاه عالم، سلانغور، ماليزيا.

²معهد العلوم، جامعة مارا للتكنولوجيا (UiTM) ، 40450 شاه عالم، سلانغور، ماليزيا.

³مركز الدراسات التأسيسية، جامعة مارا للتكنولوجيا، فرع سلانغور، حرم دنفكل، 43800 دنفكل، ماليزيا.

⁴قسم التكنولوجيا والهندسة، مجلس المطاط الماليزي، 47000 سونغاي بولو، سلانغور، ماليزيا.

الملخص

تُعد تقنية الغزل الكهربائي من التقنيات متعددة الاستخدامات والواسعة الانتشار في إنتاج الألياف النانوية ذات الشكل المورفولوجي المتحكم به والمساحة السطحية العالية، وهي خصائص جوهرية لتطبيقات الترشيح والهندسة الطبية الحيوية والمستشعرات. ويلعب اختيار المذيب دوراً محورياً في تحديد كفاءة عملية الغزل الكهربائي وخصائص الألياف الناتجة. في هذه الدراسة، تم تصنيع ألياف نانوية من بولي(ميثيل ميثاكريلات) (PMMA) باستخدام تقنية الغزل الكهربائي عبر أربعة مذيبات مختلفة: رباعي هيدرو الفوران (THF)، ثنائي ميثيل الفورماميد (DMF)، الكلوروفورم (CHCl₃)، والأسيتون، بتركيز بوليمري يبلغ 20% (وزن/وزن). كشفت اختبارات التوتر السطحي أن DMF أظهر أعلى توتر سطحي بقيمة 40.11 mN/m، مما أثر في تكوين الألياف. كما جرى تحسين معاملات الغزل الكهربائي، وتم توصيف الألياف النانوية باستخدام المجهر الإلكتروني الماسح بانبعث الحقل (FESEM) ومجهر القوة الذرية (AFM). أكد FESEM أن أقطار الألياف النانوية تراوحت بين 100 نانومتر و700 نانومتر، حيث سجلت ألياف DMF أصغر متوسط قطر (~150 نانومتر). وأظهر تحليل AFM أن ألياف PMMA المنتجة باستخدام DMF تمتلك أعلى خشونة سطحية، ويُعزى ذلك إلى خصائص المذيب. تُظهر هذه النتائج أن DMF هو المذيب الأكثر فعالية من بين المذيبات المختبرة لإنتاج ألياف PMMA نانوية دقيقة ذات مورفولوجيا مميزة وخصائص سطحية محسنة، مما يبرز التأثير الحاسم لاختيار المذيب في تصنيع الألياف النانوية بالغزل الكهربائي.

الكلمات المفتاحية: الغزل الكهربائي، ألياف نانوية، بولي(ميثيل ميثاكريلات)، مذيبات، التوتر السطحي.